PACS numbers: 42.55.Rz; 42.55.Xi; 42.60.Fc; 42.65.Re
DOI: 10.1070/QE2012v042n04ABEH014801

High-power efficient cw and pulsed lasers based on bulk Yb : KYW crystals with end diode pumping

G.H. Kim, J. Yang, D.S. Lee, A.V. Kulik, E.G. Sall', S.A. Chizhov, V.E. Yashin, U. Kang

Abstract. **End-diode-pumped lasers based on one and two Yb : KYW crystals operating in cw and *Q*-switched regimes, as well as in the regime of mode-locking, are studied. The single-crystal laser generated stable ultrashort (shorter than 100 fs) laser pulses at wavelengths of 1035 and 1043 nm with an average power exceeding 1 W. The average output power of the two-crystal laser exceeded 18 W in the cw regime and 16 W in the *Q*-switched regime with a slope efficiency exceeding 30 %.**

Keywords: *solid-state lasers, diode pumping, femtosecond pulses.*

1. Introduction

The ytterbium-doped tungsten crystals $Yb^{3+}:KY(WO_4)_2$ (Yb : KYW) and $Yb^{3+}:KGd(WO_4)_2$ (Yb : KGW) are currently widely used to develop diode-pumped lasers operating in a wavelength region near 1000 nm. Good optical, spectral, and luminescent properties of these materials [1, 2] allow one to create efficient cw or nanosecond pulsed lasers [1, 3, 4], while the broad luminescence band provides an additional possibility of generating and amplifying pulses with durations of 100–300 fs (see, for example [2, 5–8]). These crystals have different optical, spectral, and luminescent parameters along different crystallographic (*a*, *b*, *c*) and optical (N_m, N_p, N_g) axes [9], which makes it possible to control the absorption of pump radiation, as well as the polarisation and the spectral width (and, hence, the duration) of generated or amplified ultrashort pulses [10]. With respect to the thermal conductivity (~3.3 W m^{-1} K^{-1}), tungstates [9, 11] take an intermediate position between garnets and glasses, which allows one to obtain radiation with rather high average powers.

This work is devoted to the experimental study of cw and pulsed (nano- and femtosecond) end-diode-pumped Yb : KYW lasers. Special attention is paid to the efficiency of conversion of the laser diode radiation to the output radiation, as well as to the formation of shortest possible femtosecond pulses. To achieve these goals, one needs to optimise both the pump parameters and the conditions of generation of ultrashort pulses.

G.H. Kim, J. Yang, D.S. Lee, A.V.Kulik, E.G. Sall', SA.Chizhov, U. Kang KERI, Russia Science Seoul, 612, DMC, Hi-Tech Industry Center, 1580 Sangam-dong, Mapo-gu, 121-835 Seoul, Korea;
V.E. Yashin Federal State Unitary Enterprise – Scientific and Industrial Corporation 'Vavilov State Optical Institute', Birzhevaya liniya 12, 192288 St. Petersburg, Russia; e-mail: vyashin@yandex.ru

Received 8 December 2011
Kvantovaya Elektronika **42** (4) 292–297 (2012)
Translated by M.N. Basieva

Using bulk active elements in the form of rods or slabs, one can increase the average power only by increasing the length of the active medium or the number of active elements. In this connection, we studied the possibility of increasing the average power by passing from a single-crystal to a two-crystal laser scheme.

2. Single-crystal laser

The optical scheme of a single-crystal laser is shown in Fig. 1. As an active medium in this scheme, we used Yb : KYW crystals 3 × 3 × 3 mm in size with 5 at. % of Yb^{3+} ions. We used two types of crystals, namely, with optical faces perpendicular to the N_p axis (so-called N_p-cut crystals) and perpendicular to the N_g optical axis (N_g-cut crystals). Crystals with these orientations of optical axes produce laser radiation at wavelengths of 1035 and 1043 nm at the corresponding choice of the radiation polarisation with respect to the N_m and N_p axes and have different thermooptical characteristics [12, 13], which may affect the angular divergence of the laser beam. A laser crystal wrapped with indium foil was mounted in a copper heatsink cooled by running water. The optical surfaces of the crystals were antireflection coated for both the pump (λ = 981 nm) and output (λ = 1035–1043 nm) wavelength, and the edges of the crystals were bevelled at an angle of 30′ to avoid possible modulation of the spectrum.

The laser crystals were pumped by a fibre-coupled (output diameter 100 μm, numerical aperture NA = 0.11) 10-W laser diode. To retain the linear output polarisation, which is necessary for efficient pumping of Yb : KYW, the initial fibre length (100 cm) was decreased to approximately 10 cm. For precise matching of the incident pump beam polarisation with

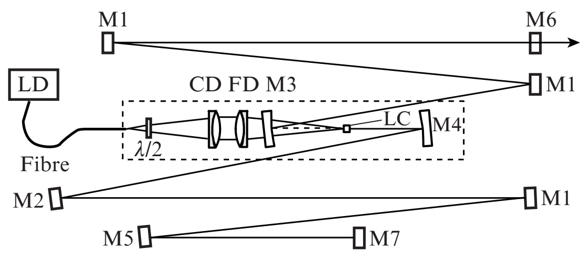

Figure 1. Optical scheme of a single-crystal laser: (LC) Yb : KYW laser crystal; (CD) and (FD) achromatic doublets collimating and focusing the pump beam; (M1) plane chirped mirrors; (M2) plane mirror; (M3) concave dichroic mirror; (M4) concave dielectric mirror; (M5) concave dielectric mirror; (M6) output mirror; (M7) semiconductor saturable mirror (SAM); (LD) semiconductor laser diode.

the N_m axis corresponding to the maximum absorption of the crystal, a half-wave plate was introduced into the scheme.

The laser diode was placed on a water-cooled thermoelectric Peltier element. Such a design allowed us to tune the diode wavelength to the laser crystal absorption maximum (~981 nm). The pump beam from the fibre output was collimated by an achromatic doublet with the focal length $F_1 = 60$ mm and, through a dichroic mirror with a transmittance of 90%–95%, focused into the laser crystal volume by another achromatic doublet with the same focal length. The pump spot diameter was 100 μm, which made it possible to reliably overcome the transparency threshold, which is approximately 3 kW cm^{-2} for Yb:KYW crystals. The total losses of the pump power on the dichroic mirror and on the elements of the forming optical system were about 14%.

To match the transverse dimensions of the pumped region with the cavity mode size, which is necessary for efficient lasing, we selected the focal length of the spherical cavity mirrors focusing the generated radiation into the laser crystal and slightly shifted the active element along the longitudinal axis with respect to the caustic. Calculations using the LASCAD software [14] showed that a crystal in the cavity of this configuration must be positioned with an accuracy of about 0.5 mm.

An output mirror with a transmittance of 8% was placed in the left arm of the cavity. From calculations performed using the above software, we concluded that the output laser power for mirrors with transmittances of 4%–10% is almost constant. In the second arm of the cavity, a concave mirror with the curvature radius $R = 300$ mm focused the laser beam on a mirror. As the latter, we used an ordinary highly reflecting dielectric mirror in the case of cw operation and a semiconductor saturable absorber mirror (SESAM or SAM) [15] with the initial absorption A_0 = 1%–4% in the regime of mode-locking. The radius of curvature of the focusing mirror was chosen so that the radiation intensity on the SAM exceeded the absorber saturation intensity.

As is well known [16], to obtain pulses shorter than 1 ps in a femtosecond laser cavity, it is necessary to compensate the dispersion in the active laser element. For this purpose, it is most convenient to use chirped mirrors [17]. In this case, the scheme becomes more compact than when using a prism delay line because the dispersion compensation does not depend on the distance between the mirrors and is determined only by the dispersion introduced by the mirrors. Because of this, we used in the laser three chirped mirrors with the total single-pass group velocity dispersion GDV = –1350 fs^2, which is approximately equal to the positive dispersion introduced by the active element.

The dependences of the output laser power on the pump power incident on the crystal in the free-running regime are given in Fig. 2. The maximum output power exceeded 1.6 W for both orientations of the crystal. The slope and optical efficiencies in this case were equal to 48%–54% and 32%, respectively, with respect to the pump power incident on the crystal. Note that, for quasi-four-level laser materials, it is difficult to experimentally estimate the absorbed pump power due to the absorption saturation typical for these media. Therefore, to estimate the laser efficiency, we took into account the incident pump power, although the use of this parameter instead of the absorbed power leads to underestimation of the real lasing efficiency.

To obtain the ultrashort pulse regime, we used semiconductor saturable absorber mirrors (SAMs) as highly reflecting mirrors. Our experiments showed that the most stable (without instability caused by undesirable Q-switching [18]) operation of the laser was observed when a mirror with the initial absorption $A_0 > 2\%$ was used.

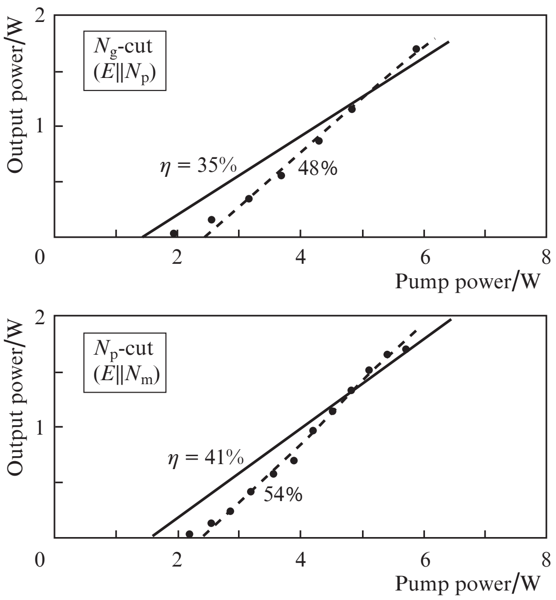

Figure 2. Dependences of the output laser power in the cw regime on the incident pump power for Yb:KYW crystals with different orientations. The solid line is calculated by the LASCAD program and the dashed line shows the linear approximation of experimental points.

In this regime, at an average output power of 700–1000 mW and a pulse repetition rate of 78.7 MHz, the energy of a single femtosecond pulse exceeded 10 nJ. Figure 3 shows the autocorrelation function and the spectrum of femtosecond laser pulses for N_g- and N_p-cut crystals. One can see that the spectra of the crystals with these orientations are centred at wavelengths of 1043 and 1035 nm, the FWHMs of these spectra are 12.5 and 9.0 nm, and the pulse durations are 90 and 110 fs, respectively. The products of the spectral widths and pulse durations for these crystals exceed this product for pulses with sech^2 intensity profiles [16] approximately by a factor of 1.1. These data, as well as the data of FROG [19], show that the generated femtosecond pulses are almost free of frequency modulation (chirp), while the rather small pulse durations are caused, in our opinion, by the joint effect of the Kerr nonlinearity and the saturable absorber and by the formation of the so-called soliton regime of operation [20].

The transverse profile of the output beam intensity recorded by a CCD camera at a distance of 20 cm from the output mirror shows that the beams have a good axial symmetry with a bell-like intensity distribution. We also measured the spatial-angular characteristics of the output beam, i.e., the beam quality parameter M^2 [16, 21]. This parameter was calculated from the measured evolution of the laser beam diameter during the beam propagation; for two mutually perpendicular directions, we had $M_x^2 = 1.07$ and $M_y^2 = 1.1$, which is rather close to $M^2 = 1$ of the ideal Gaussian beam. A slight astigmatism of the beam with the ratio of the ellipse axes of about 1.03 is associated with an inclination of the spherical dichroic mirrors. The beam quality parameter was almost the same in the femtosecond pulse and cw regimes in the entire region of output powers. A difference in possible thermooptical distortions related to the crystal orientations (N_g and N_p)

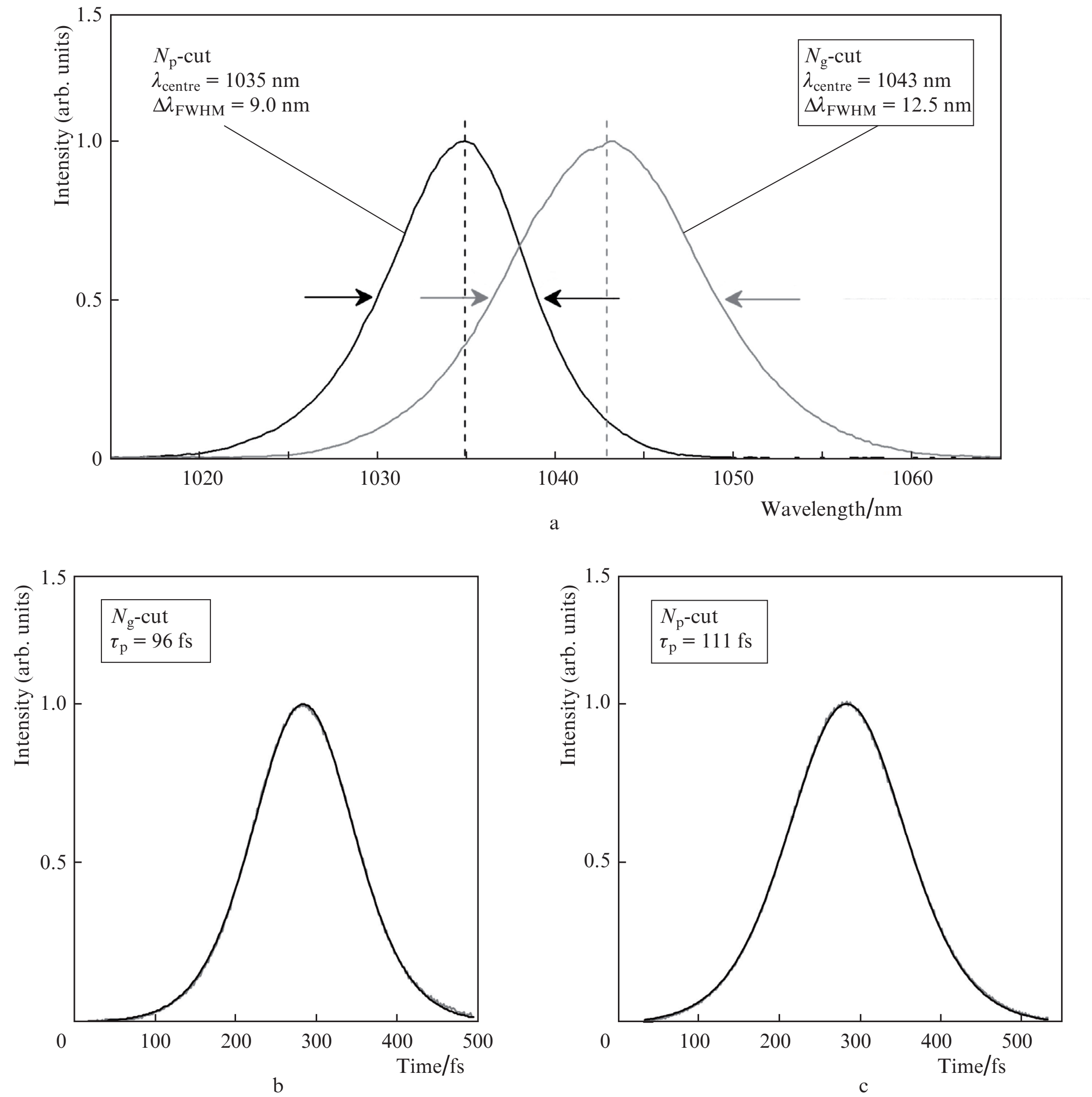

Figure 3. Spectra (a) and autocorrelation functions (b, c) of femtosecond laser pulses for N_g- and N_p-cut crystals.

[12] also had no influence on the beam quality, which can be explained by a relatively low pump power. For example, estimates based on the available literature data [22, 23] and our calculations using the LASCAD software yield the thermooptical lens with a focal length of 180–200 cm.

We also measured the output power stability in the cw regime. These measurements revealed that the laser power was stable within 0.3% during more than 2 h after an approximately 30-min stabilisation. The laser beam direction stability measured with a CCD camera lied within 0.3%–0.5% and 1.2%–1.9% for the horizontal and vertical directions, respectively, with respect to the diffraction divergence of the output laser beam.

In addition, we studied a single-crystal laser with a slightly changed optical scheme and a higher pump power [24]. In this scheme, the pump radiation with a power up to 25 W was collimated and focused into the laser crystal volume through a plane dichroic mirror to a spot about 160 μm in diameter. The maximum average power of this laser in the cw regime reached 4.1 W at an incident pump power of 20 W and a slope efficiency of 40%. The output power in the self-mode-locking regime was 3.5 W at a pulse repetition rate of 85.5 MHz, which gives a single pulse energy exceeding 30 nJ. The duration of pulses in the train was 200 fs, which indicates that the self-mode-locking occurs only due to the action of the saturable absorber and a weak action of the self-modulation and the Kerr lens. This was obviously related to a larger mode size than in the case of a lower-power laser. Despite a higher average power, this laser generated high-quality beams without noticeable influence of thermooptical effects.

The obtained parameters make it possible to use the developed lasers both as independent sources (for example, for generation of terahertz radiation or for micro-modification of materials) and as master oscillators of high-power laser systems.

3. Two-crystal laser

As was mentioned above, the maximum average power of solid-state lasers is limited either by the thermal destruction of the active medium or by thermooptical aberrations [25]. Therefore, one of a few methods of increasing this power in the case of bulk laser media is to increase the active medium length or to use several active elements in the cavity. To increase the average laser power and simultaneously to retain the high spatial quality of the output beam, we used a scheme with two active elements (see also [10, 26]).

The optical scheme of a laser with two active elements made of Yb:KYW crystals with different orientations of optical axes is shown in Fig. 4. The use of N_p- and N_g-cut crystals, which have different spectral and luminescent characteristics at a corresponding orientation of the polarisation vector of generated or amplified beams, makes it possible to widen the gain band and thus generate or amplify more broadband chirped or femtosecond pulses [10]. The crystals were 5 mm long and contained 3% of ytterbium ions, which ensured a good (above 70%) absorption of the pump radiation. Similar to the case of the single-crystal laser, the pump beam and cavity mode sizes were matched by a longitudinal shift of the active elements. To eliminate possible modulation of the spectrum, the faces of the active elements were antireflection coated and inclined at an angle of $\sim 30'$. As pump sources, we used two fibre-coupled laser diode arrays with a power of 50 W each. The depolarisation of the pump radiation was minimised using a short (30 cm) optical fibre 200 μm in diameter with the numerical aperture NA = 0.22. The pump beams from the fibre output were collimated and focused through dichroic mirrors into the active crystal to a spot with a diameter of about 320 μm, which is close to the diameter of the TEM_{00} cavity mode. This mode was calculated by the well-known matrix method taking into account the astigmatic thermal lenses induced in the active elements by the pump radiation. Using the LASCAD software, the focal length of these lenses was calculated to be 480–550 mm for the N_p-cut crystal at an incident power of 30 W. These values are in adequate agreement with the literature data [22, 23].

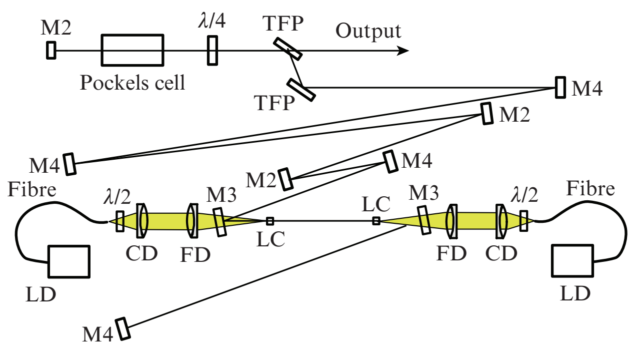

Figure 4. Optical scheme of a two-crystal laser: (TFP) thin-film dielectric polarisers; the other symbols are the same as in Fig. 1.

As an output mirror in this scheme, we used a thin-film polariser in combination with a quarter-wave plate, which was rotated to obtain the maximum output power at a given pump power. For electrooptic Q-switching, we used a Pockels cell based on a BBO crystal and controlled by a special unit. The pulse repetition rate was smoothly changeable from single pulses to 500 kHz.

The output laser power in the cw regime in the cases of using single active elements and two elements simultaneously is shown in Fig. 5 versus the pump power incident on the crystals. The maximum output power was 12.5 and 9 W at a slope efficiency of 47% and 37% for N_g- and N_p-cut single crystals, respectively. Note that the output powers for the crystal in which the polarisation vector of the laser beam is parallel to the N_p axis ($E \| N_p$) are higher than for the crystal with $E \| N_m$ despite a smaller stimulated emission cross section [9]. This behaviour of power can be explained, in our opinion, by different spectral losses in the cavities with crystals emitting at different wavelengths. The maximum output power in the case of two crystals in the cavity was 18.5 W at a pump power of 72 W, which yields the total and slope efficiencies of 25% and 35%, respectively. The laser radiation spectrum was centred at a wavelength of 1035 nm, and its width did not exceed 1 nm.

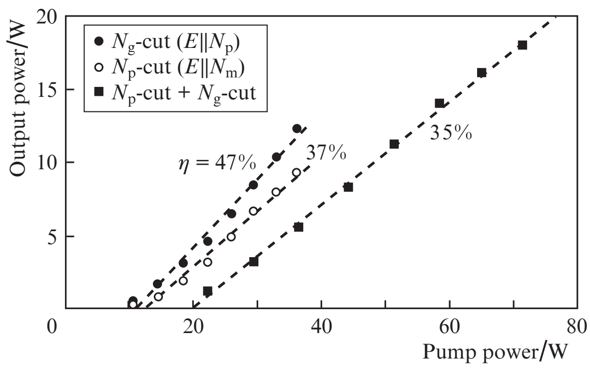

Figure 5. Average output power of a two-crystal laser in the cw regime in the cases of separate and common operation of crystals versus the incident pump power.

Note that the output laser power was maximised in measurements for each pump power by optimal adjustment of the quarter-wave plate. As can be easily shown, this measurement method leads to an underestimation of the slope efficiency. It is this fact that can explain the considerable difference in the slope efficiencies of single- and two-crystal lasers at close total efficiencies (27%–30% and 25%, respectively).

The maximum output power obtained in the case of Q-switching reached 16 W at a pulse repetition rate of 100 kHz and 14 W at a repetition rate of 500 kHz (Q-switching time 800 ns). This decrease in the average power with respect to the free-running regime can be explained by additional losses introduced by the electrooptic Q-switch. As the Q-switching time decreased to 400 ns, the output power decreased by three times, which obviously occurred because this time was too short for oscillation development. The output pulse duration, determined mainly by a rather long length of the cavity, was 20 ns. The width of the spectrum was 16 nm, which points to a pronouncedly multimode regime. The spectrum had two peaks, at wavelengths of 1035 and 1043 nm, which correspond to the spectral maxima of the gain coefficient for the two used crystals.

Multicrystal lasers with a high average power can be used both for generation of high-power femtosecond pulses [27] and for their regenerative amplification [10]. The second, more flexible approach to the creation of high-power femtosecond lasers, is more advantageous in some cases, since this allows one to obtain shorter femtosecond pulses and considerably decrease the pulse repetition rate (to hundreds of kilohertz), which is important for some technical applications. We used the above-described two-crystal resonator as a regenerative amplifier of the radiation of a single-crystal master oscillator [28]. After optimisation of the resonator parameters, we obtained the radiation parameters listed below. The average power reached 14 W at the exit from the amplifier and 8.7 W after passing through a compressor at a pulse duration of 180 fs (in the case of modification of the pulse spectrum at the entrance), which resulted in a peak power exceeding 200 MW at a pulse repetition rate of 200 kHz. The laser was able to operate with a pulse repetition rate up to 500 kHz with approximately the same average power.

Maximum average output power of the regenerative amplifier/W	14
Energy of a single femtosecond pulse in μJ after passing. a compressor at a pulse repetition rate of	
50 kHz	160
500 kHz	16
Pulse duration at the exit of the	
regenerative amplifier/ps	50
compressor/fs	180
Beam quality	$M^2 < 1.2$

It should be noted that the energy of amplified ultrashort laser pulses in laser crystals can be limited by different physical processes, such as optical breakdown, self-action, stimulated scattering, and multiphoton processes [25]. A specific feature of KGW/KYW crystals is a high Raman gain coefficient [9, 29], which, on the one hand, allows one to create efficient Raman lasers and, on the other hand, is an obstacle for the formation of ultrashort pulses with a sufficiently high energy [30]. In particular, in our case, we observed the first and second Stokes components of SRS (λ_1 = 1145 nm and λ_2 = 1270 nm) with a frequency shift of 901 cm^{-1} when amplifying chirped pulses with a duration of 50 ps, an energy of 160 μJ, and a repetition rate of 50 kHz, from which the Raman gain coefficient is estimated as $g \approx 1.1$ cm GW^{-1}. This value considerably differs from the stationary coefficient $g_{st} \approx$ 4 cm GW^{-1} [29], which is related to a large spectral width of chirped pulses (~10 nm), exceeding the Raman line width (~6 nm). As is known [25], the SRS excitation efficiency in this case strongly decreases.

For most applications of femtosecond pulses, which require high power densities, it is important to have a high spatial quality of the beam. We measured the beam quality with a CCD camera. The recorded intensity distribution in the near-field zone showed that, at a high output power (exceeding 10–12 W at the exit of the amplifier), the beam quality is deteriorated, i.e., one observes astigmatic distortions of the spot shape. At the same time, the measurements showed that the beam retains the axial symmetry up to a power of about 12 W at a pulse repetition rate of 500 kHz and approximately up to 10 W at 100 kHz. In this case, the measured beam quality parameter was $M_x^2 \times M_y^2$=1.19 × 1.24. At pulse repetition rates below 50 kHz, the beam quality may already be affected by SRS.

4. Conclusions

In this work we studied lasers and amplifiers based on Yb:KYW/Yb:KGW crystals and operating both in the cw regime and in the regime of lasing and amplification of nanosecond and picosecond pulses. The use of several active elements in one cavity allows us to scale the average power of such lasers and retain a high laser beam quality. In particular, in the case of a two-crystal scheme, we obtained average powers of 18, 16, and 14 W for cw and single-pulse regimes and amplification of chirped picosecond pulses, respectively. Our two-crystal scheme with spectrally shifted gain coefficient maxima of the crystals also allowed us to amplify broadband chirped pulses without pronounced distortions of the spectrum, which made it possible to shorten the output amplifier pulses to 180 fs. The energy of amplified pulses is SRS-limited at a level of 160 μJ.

Despite the fact that the highest average powers of femtosecond laser pulses were obtained using active elements in the form of a thin disk [11, 31] or a slab [32], lasers with bulk active elements also have a right to exist and allow scaling of their average power. This is related to their relatively simple design and a low cost of laser modules, which can be produced without complicated technological methods and are free of problems related to mounting of thin active elements (as in the case of thin disks) or to using complex multipass amplification schemes needed for slabs.

Acknowledgements. This work was supported by the Seoul R&BD Program (Contract No. WR100001).

References

1. Kuleshov N.V., Lagatsky A.A., Podlipensky A.V., Mikhailov V.P., Huber G. *Opt. Lett.*, **22**, 1317 (1997).
2. Kisel' V.E., Troshin A.E., Shcherbitskii V.G., Kuleshov N.V., Pavlyuk A.A., Brunner F., Paschotta R., Morier-Genoud F., Keller U. *Kvantovaya Elektron.*, **36** (4), 319 (2006) [*Quantum Electron.*, **36** (4), 319 (2006)].
3. Lagatsky A.A., Kuleshov N.V., Mikhailov V.P. *Opt.Commun.*, **165**, 71 (1999).
4. Grabchikov A.S., Kuz'min A.N., Lisinetskii V.A., Orlovich V.A., Voinovich A.P., Demidovich A.A., Eichler H.J., Titov A.N. *Kvantovaya Elektron.*, **33** (2), 165 (2003) [*Quantum Electron.*, **33** (2), 165 (2003)].
5. Brunner F., Spuhler G.J., Aus der Au J., Krainer L., Morier-Genoud F., Paschotta R., Lichtenstein N., Weiss S., Harder C., Lagatsky A.A., Abdolvand A., Kuleshov N.V., Keller U. *Opt. Lett.*, **25**, 1119 (2000).
6. Brunner F., Sudmeyer T., Innerhofer E., Morier-Genoud F., Paschotta R., Kisel V.E., Shcherbitsky V.G., Kuleshov N.V., Gao J., Contag K., Giesen A., Keller U. *Opt. Lett.*, **27**, 1162 (2002).
7. Major A., Cisek R., Barzda V. *Opt. Express*, **14**, 12163 (2006).
8. Kim G.H., Kang U., Heo D., Yashin V.E., Kulik A.V., Sall' E.G., Chizhov S.A. *Opt. Zh.*, **77** (4), 3 (2010).
9. EKSPLA, www.ekspla.com.
10. Buettner A., Buenting U., Wandt D., Neumann J., Kracht D. *Opt. Express*, **18**, 21973 (2010).
11. Sudmeyer T., Krankel C., Baer C.R.E., Heckl O.H., Saraceno C.J., Golling M., Peters R., Petermann K., Huber G., Keller U. *Appl. Phys. B*, **97**, 281 (2009).
12. Loiko P.A., Yumashev K.V., Kuleshov N.V., Savitski V.G., Calvez S., Burns D., Pavlyuk A.A. *Opt. Express*, **17**, 23536 (2009).
13. Chenais S., Balembois Druon F., Lucas-Leclin G., Georges P. *IEEE J. Quantum Electron.*, **40**, 1217 (2004).
14. LAS-CAD GmbH, www.las-cad.com.
15. Keller U., Miller D.A.B., Boyd G.D., Chiu T.H., Ferguson J.F., Asom M.T. *Opt. Lett.*, **17**, 505 (1992).
16. Diels J.-C., Rudolph W. U*ltrashort Laser Pulse Phenomena: Fundamentals,Ttechniques, and Applications on Femtosecond Time Scale* (Boston: Acad. Press, 2006).
17. Szipocs R., Ferencz K., Spielmann C., Krausz F. *Opt. Lett.*, **19**, 201 (1994).
18. Honninger C., Paschotta R., Morier-Genoud F., Moser M., Keller U. *J. Opt. Soc. Am. B*, **16**, 46 (1999).
19. Swamp Optics, www.swampoptics.com.

20. Kartner F.X., Keller U. *Opt. Lett*., **20**, 16 (1995).
21. Potemkin A.K., Khazanov E.A. *Kvantovaya Elektron*., **35** (11), 1042 (2005) [*Quantum Electron*., **35** (11), 1042 (2005)].
22. Biswal S., O'Connor S.P., Bowman S.R. *Appl. Opt*., **44**, 3093 (2005).
23. Chenais S., Druon F., Forget S., Balembois F., Georges P. *Progr. Quantum Electron*., **30**, 89 (2006).
24. Kim G.H., Kang U., Heo D., Yashin V.E., Kulik A.V., Sall' E.G., Chizhov S.A. *Opt. Spektrosk*., **108**, 861 (2010).
25. Mak A.A., Soms L.N., Fromzel' V.A., Yashin V.E. *Lazery na neodimovom stekle* (Neodymium-Glass Lasers) (Moscow: Nauka, 1990).
26. Stučinskas D., Antipenkov R., Varanavičius A. *Proc. SPIE Int. Soc. Opt. Eng*., **6731**, 67312Y-1 (2007).
27. Palmer G., Schultze M., Emons M., Lindemann A.L., Pospiech M., Steingrube D., Max Lederer D., Morgner U. *Opt. Express*, **18**, 19095 (2010).
28. Kim G.H., Yang J., Chizhov S.A., Sall E.G., Kulik A.V., Yashin V.E., Lee D.S., Kang U. *Opt. Express*, **20**, 3434 (2012).
29. Basiev T.T. *Fiz. Tv. Tela*, **47**, 1354 (2005).
30. Liu H., Nees J., Mourou G., Biswal S., Spuhler G.J., Keller U., Kuleshov N.V. *Opt. Commun*., **203**, 315 (2002).
31. Baer C.R.E., Kränkel C., Saraceno C.J., Heckl O.H., Golling M., Peters R., Petermann K., Südmeyer T., Huber G., Keller U. *Opt. Lett*., **35**, 2302 (2010).
32. Russbueldt P., Mans T., Weitenberg J., Hoffmann H.D., Poprawe R. *Opt. Lett*., **35**, 4169 (2010).